This article was downloaded by: [Tomsk State University of Control Systems and Radio]
On: 18 February 2013, At: 10:08
Publisher: Taylor & Francis
Informa Ltd Registered in England and Wales Registered Number: 1072954 Registered office: Mortimer House, 37-41 Mortimer Street, London W1T 3JH, UK

Molecular Crystals and Liquid Crystals Science and Technology. Section A. Molecular Crystals and Liquid Crystals
Publication details, including instructions for authors and subscription information:
http://www.tandfonline.com/loi/gmcl19

Dynamic Phenomena in Organic Metal $(BEDT\text{-}TTF)_3Ta_2F_{11}$

Juana Vivó Acrivos [a]
[a] San José State University, San José, CA, 95192-0101
Version of record first published: 24 Sep 2006.

To cite this article: Juana Vivó Acrivos (1996): Dynamic Phenomena in Organic Metal $(BEDT\text{-}TTF)_3Ta_2F_{11}$, Molecular Crystals and Liquid Crystals Science and Technology. Section A. Molecular Crystals and Liquid Crystals, 284:1, 411-417

To link to this article: http://dx.doi.org/10.1080/10587259608037943

PLEASE SCROLL DOWN FOR ARTICLE

Full terms and conditions of use: http://www.tandfonline.com/page/terms-and-conditions

This article may be used for research, teaching, and private study purposes. Any substantial or systematic reproduction, redistribution, reselling, loan, sub-licensing, systematic supply, or distribution in any form to anyone is expressly forbidden.

The publisher does not give any warranty express or implied or make any representation that the contents will be complete or accurate or up to date. The accuracy of any instructions, formulae, and drug doses should be independently verified with primary sources. The publisher shall not be liable for any loss, actions, claims, proceedings, demand, or costs or damages whatsoever or howsoever caused arising directly or indirectly in connection with or arising out of the use of this material.

Mol. Cryst. Liq. Cryst., 1996, Vol. 284, pp. 411–417
Reprints available directly from the publisher
Photocopying permitted by license only

© 1996 OPA (Overseas Publishers Association)
Amsterdam B.V. Published in The Netherlands
under license by Gordon and Breach Science
Publishers SA
Printed in Malaysia

Downloaded by [Tomsk State University of Control Systems and Radio] at 10:08 18 February 2013

DYNAMIC PHENOMENA IN ORGANIC METAL $(BEDT\text{-}TTF)_3Ta_2F_{11}$

JUANA VIVÓ ACRIVOS
San José State University, San José, CA 95192-0101

Abstract Dynamic electron spin resonance, ESR measurements suggest that this paramagnetic, layered organic metal behaves similarly to cuprate superconductors. There is a dynamic equilibrium between doublet, D and triplet, T* states near the transition temperature to superconductivity T_c= 10±3 K; antiferromagnetic, AF resonance is observed from room temperature to ≈ 150 K, in this temperature region the temperature dependence of the D Lorentzian ESR line widths obtains a first order rate constant for the disappearance of the state ($k_1 = 3.5 \times 10^7 e^{-111/T}$/s) and T* ESR is not observed, it is detected only below 44 K when the lifetime of AF domains, τ_{AF} decreases below 10^{-10}s; the onset of superconductivity is ascertained by the appearance of an energy loss at exactly H=0 near 10 K and by the magnetization oscillations observed versus H below T_c when the samples are cooled in a non-zero field H; the fourfold increase in the relaxation time τ_1 for the half field T* ESR absorption near 10 ±3 K is interpreted using the Gorter phenomenological relation $\tau_1=C_H/\alpha_H$, C_H and α_H are the heat capacity and lattice thermal contact coefficient of the spin system, at H.

INTRODUCTION

In this work, the transition to superconductivity of a paramagnetic organic metal $(BEDT\text{-}TTF)_3Ta_2F_{11}$,[1] is ascertained from the onset of the energy loss at H=0 and magnetization jumps due to flux pinning, observed when the samples are cooled below T_c in H≠0. The magnetic response includes the detection of D, T* ESR, AF resonance, energy loss and magnetization oscillations in the superconducting state.[2] The ESR relaxation time $\tau_1(T_c)$ is related to thermodynamics by the Gorter,[3] relation:

$$\tau_1 = C_H/\alpha_H, \qquad (1)$$

C_H and α_H are respectively the heat capacity and the thermal contact coefficient to the lattice of the spin system, at constant field H. The spin system temperature T_S approaches the lattice temperature T_0 as:

$$dT_S/dt = (T_0-T_S)/\tau_1, \text{ when } |T_0-T_S|/T_0 \ll 1. \qquad (2)$$

The organic free radical cations (S=1/2) are aligned to maximize the chalcogen, π-π intermolecular interactions (Figure 1a).[1] These charged free spin species interact with

the lattice vibrations to produce a polarization, called a polaron.[4] Alaxandrov and Mott[5] have shown that such charged carriers with spin S=1/2 in a many-electron system, strongly coupled to the lattice vibrations, can tunnel to form a charged Bose-liquid of small bipolarons with charge 2e and S= 0 or 1. The Alexandrov and Mott theory is used to relate the formation of a triplet state condensate and the appearance of the sample superconductivity when the Gorter relation (1) is applied to the half field T* ESR lattice relaxation times τ_1, in order to ascertain whether the triplet state of the condensate is directly involved in the transition to superconductivity.

Downloaded by [Tomsk State University of Control Systems and Radio] at 10:08 18 February 2013

EXPERIMENTAL

Single crystals (grown at IBM) were measured at SJSU with an x-band Bruker-ER300/Oxford-900 spectrometer/cryogenic system described earlier.[1] Figures 1 and 2 show the power absorption derivative dP/dB_z response to the field $k(B_z+2B_{zm}\cos(2\pi\nu_m)) + 2iB_1\cos(2\pi\nu)$ versus B_z and temperature T from 280 K down to 3.7 K when $B_1 \parallel$ a $\perp B_z$ (Figure 1a) where B_z is the external dc field modulated with an amplitude B_{zm} at $\nu_m = 10^5$Hz, $B_1 = B_{10}10^{-dB/20}$, $B_{10} \leq 0.1$mT is the microwave field at ν = 9.36 GHz. We measure the energy loss in the superconducting state at exactly H=0,[6] the ESR near g=2.00 (D and T*, $\Delta S_z=\pm1$) and, near the half field resonance (T*, $\Delta S=0$), AF resonance,[6a,b] and magnetization oscillations,[7c] when $H\neq0$ through T_c.

DISCUSSION OF RESULTS

Four types of magnetic response are identified in Figure 1 by their orientation dependence in the external magnetic field:[2, 6a,b, 7c] ESR of D and T* states versus temperature and microwave power; AF resonance,[6a,b] identifying the direction and magnitude of the axial anisotropy field. B_A(=220 mT) $\parallel$ b-axis in the AF domains and the field produced by exchange interactions $B_E = 130.7 \pm 10$ mT; the onset of the energy loss at exactly H=0 identifies T_c,[6] by the appearance of a signal of opposite polarity to the ESR at that temperature; another signature of superconductivity observed is the appearance of magnetization jumps, due to flux pinning,[7c] when the samples are cooled in $H\neq0$ through T_c, they disappear when the samples are cooled through T_c in zero field. The D ESR lineshapes are Lorentzian/Gaussian above/below 150 K (Figure 2) and the fourfold increase in τ_1 for the T* half field ESR ($B_{z,½}\approx156$ mT) occurs near the same temperature as the onset of an energy loss signal at H=0 and, magnetization oscillations when the crystal is cooled in $H\neq0$ usually associated with superconductivity. The different possible rate processes between the magnetic states are shown in Figure 3. There are five spin states split by the field in dynamic equilibrium; the ground state is a singlet S in equilibrium with the D states and the latter are in equilibrium with the T* states via the chemical reactions:[1a]

$$S \Leftrightarrow 2D \quad \text{and} \quad 2D \Leftrightarrow T^*, \tag{3}$$

with equilibrium constants:

$$K_2 = (a[D])^2/a[S] = \exp(-\Delta_{S\text{-}D}/2T),$$
$$K_3 = k_1/k_{-1} = a[T^*]/(a[D])^2 = \exp(\Delta_{T^*\text{-}D}/2T). \tag{4}$$

Downloaded by [Tomsk State University of Control Systems and Radio] at 10:08 18 February 2013

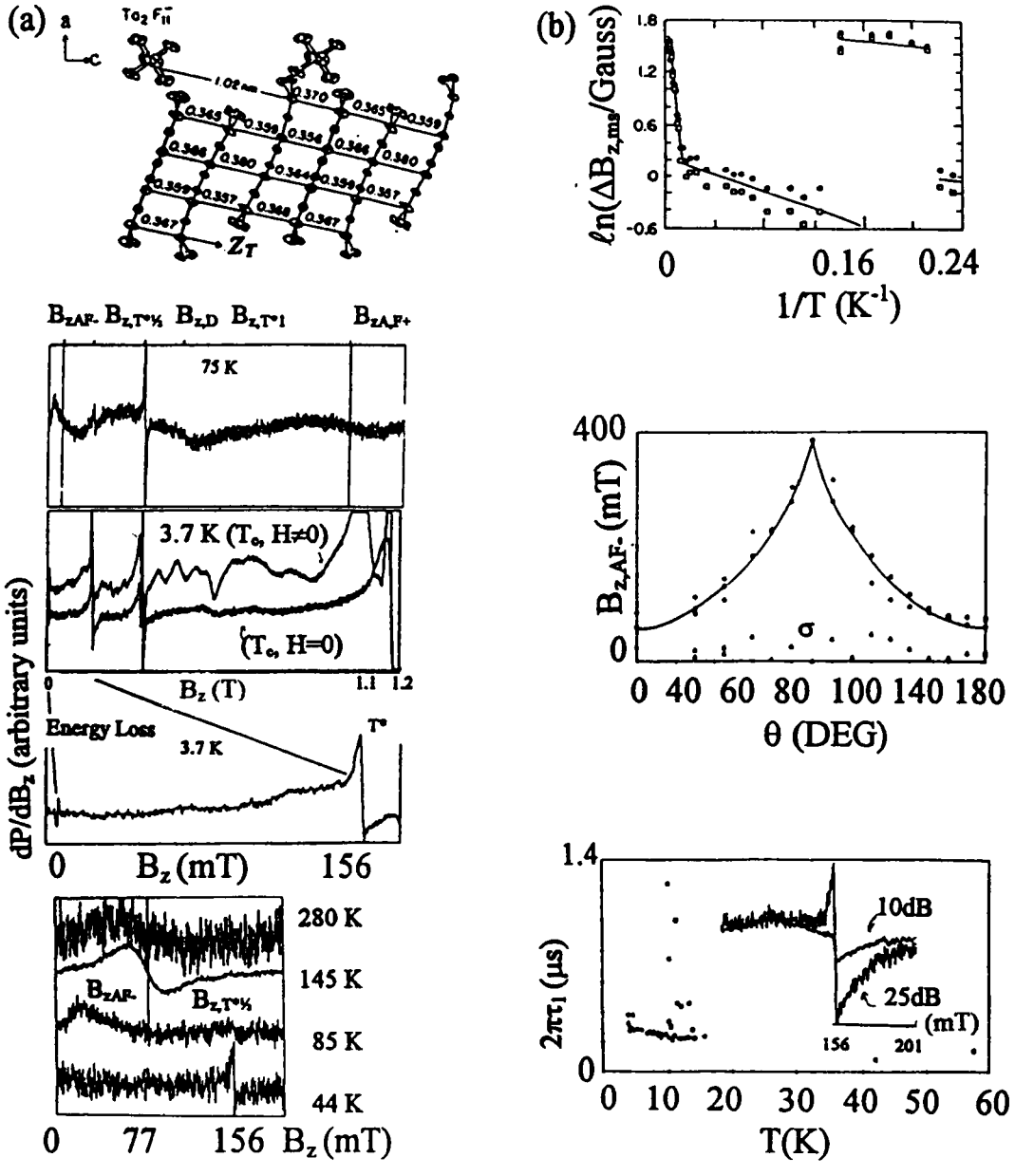

FIGURE 1 (BEDT-TTF)$_3$Ta$_2$F$_{11}$ (a) Structure and ESR data: The crystallographic parameters for the pseudo-orthorhombic lattice at room temperature are a=1.6683, b=1.1928, c=1.255 nm.[1b] The different resonance fields are identified by $B_{zAF\pm}$ for the AF domains; $B_{z,D}$, for D states and $B_{z,T^*\pm1}$, $B_{z,T^*1/2}$ for the T* states. Magnetic oscillations are observed near 3.7 K when the samples are cooled through Tc in H≠0, these are shown to disappear when the samples are cooled in H=0, determined by the position of the energy loss signal which is used to define it. (b) Data analysis: The 1/T dependence of the D ESR line width identifies at least three temperature domains of dynamic phenomena; the orientation dependence of B_{zAF-} is compared with the predicted values using the general theory,[6b] and the saturation experiments of the T* half field transition giving the values for τ_1.

The activities a[i] in relation (4) were ascertained from D, T* $\Delta S_z=\pm 1$ ESR intensity measurements, in the absence of saturation above T_c, when $a[S] \cong 1$; relation (4) obtains the temperature dependence of the band gaps: $\Delta_{S\text{-}D}/2$ and $\Delta_{T^*\text{-}D}/2$ (insert Figure 3).[1a] The rate constant k_1 is determined from the line width of the D $\Delta S_z=\pm 1$ ESR vs 1/T:[1a]

$$\Delta B_{Z,ms} = \text{constant}(k_1 + 1/T_2),$$
$$k_1 = A_0\, e^{\Delta S/R}\, e^{-\Delta U/RT}, \qquad (5)$$

where $(\Delta U/R,\ A_0 e^{\Delta S/R}) = (111\ \text{K},\ 3.5*10^7/\text{s})_{T>150\ \text{K}};\ (11\ \text{K},\ 7*10^6/\text{s})_{T<150\ \text{K}}$; ΔU and ΔS are respectively the activation energy and entropy to form activated states when D disappears. The decrease in ΔU below 150 K indicates that there is an easier path for the disappearance of D whereas the entropy increase, by $2R \approx 3R\ln 2$ above it, suggests that disorder is introduced when three possible T* states do not provide a reaction path e.g., by the two possible spin flips, each contributing Rln2 to the entropy for the three singlet states formed by antiparallel pairing, along each of the possible principal axes of triplet state formation X_T, Y_T, Z_T (Figure 1a). Near 44 K tunneling of D polarons, via lattice vibrations, pair the spins to generate S* states with 1/4 probability and, T* states with 3/4 probability; the S* states relax to the ground state S but the transition $T^* \rightarrow S$ is forbidden. All the dynamic phenomena, e.g., the population and rates of disappearance and formation of the D, S* and T* states depend on the coupling of spins to the lattice vibrations. The spin manifold (with components separated in energy by ΔE) obey a Boltzmann population distribution, i.e., $n_{|S,Sz>}/n_{|S,-Sz>} = \exp\text{-}\Delta E/k_B T_S$, where in a saturation experiment the spin temperature T_S is greater than the lattice temperature T_0, and thermal equilibrium is obtained as the Boltzmann temperature approaches T_0 according to relation (2). The ESR lifetimes depend on the chemical rates, the spin-spin and spin-lattice, and spin-radiation interactions via the transition rates $w(\Delta E)$ between the states separated by $\Delta E = h\nu$ *or* $1/2\ h\nu$ in Figure 3. It has been shown that the most efficient relaxation involves resonant phonons produced via second order Raman processes,[3] by the absorption and emission of phonons, involving an intermediate state, at frequencies ν_1 and ν_2, $\nu_2 - \nu_1 = \nu$, i.e.,

$$E_{|S,Sz>} + h\nu_{\text{radiation}} = E_{|S,-Sz>} \text{ returns to initial state by:}$$
$$E_{|S,-Sz>} + h\nu_1 = E_{\text{intermediate}};\quad E_{\text{intermediate}} - h\nu_2 = E_{|S,Sz>}. \qquad (6)$$

The phonon temperature and heat capacity (T_{ph}, C_{ph}) depend on the contact with the lattice at temperature T_0 and infinite heat capacity and, the transition rates $w(\Delta E)$ depend on the energy transfer path:

$$\text{Spin System}(T_S, C_H) \Rightarrow \text{Resonant Phonons}(T_{ph}, C_{ph}) \Rightarrow \text{Bath}\ (T_0,\ \text{Infinite Heat Capacity}),$$

$C_{ph} < C_H$ indicates that there may be a bottleneck when phonons are involved in a phase transition. The chemical dynamics for the relaxation processes in Figure 3 obtain:[2,3]

$$1/\tau_1(h\nu) = w^{=}(h\nu) + w^{++}(h\nu) + [w^{-}(h\nu/2) + w^{+}(h\nu/2)]/2 + k_{-1}. \qquad (7)$$

Downloaded by [Tomsk State University of Control Systems and Radio] at 10:08 18 February 2013

Downloaded by [Tomsk State University of Control Systems and Radio] at 10:08 18 February 2013

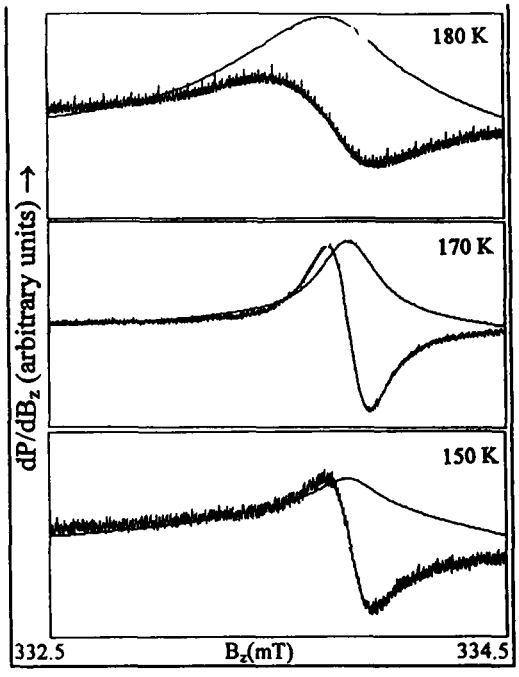

FIGURE 2 D ESR line shapes versus T. The line shapes are Lorentzian/Gaussian above/below 150 K. The field dependence of the Gaussian line (T< 150 K) obtains the spin-spin exchange interaction, according to the Anderson Weiss theory,[3] to be $J_{spin\text{-}spin} \approx 15$ mT.

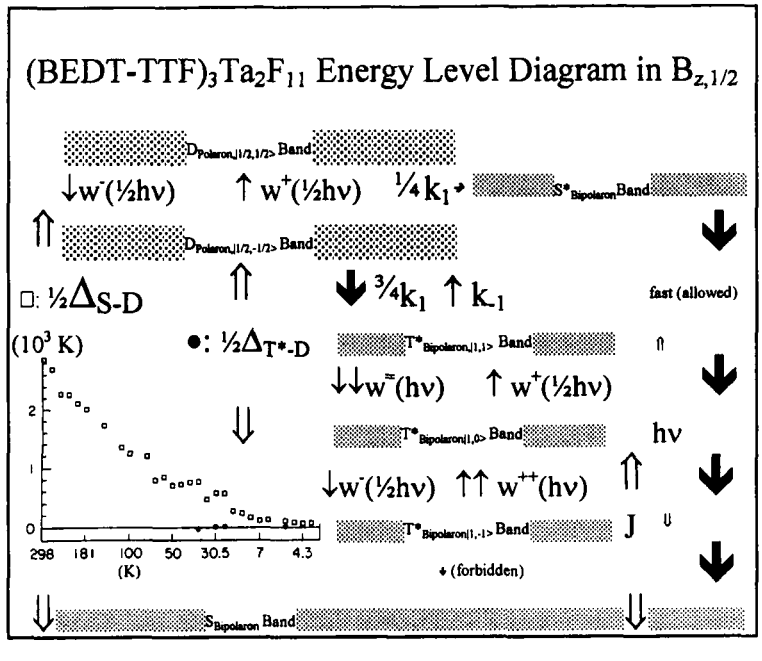

FIGURE 3 Energy level diagram. The insert gives □: ½Δ$_{S\text{-}D}$ and •: ½Δ$_{T^*\text{-}D}$ in relation (4) vs T. The fourfold τ_1 increase near 10 K (Figure 1b) suggests that a phonon bottleneck has decreased the rates w(ΔE) and that the lifetime of T* is determined most probably by 1/k$_{-1}$, which also depends on the lattice vibrations.

T_c may be associated with the τ_1 increase via the Gorter relation (1):

$$\Delta\tau_1(T_c)/\tau_1 = \Delta C_H/C_H - \Delta\alpha_H/\alpha_H \approx 4. \quad (8)$$

C_H and α are the contributions of the spin system to the thermodynamic values of the heat capacity, C_p and thermal conduction coefficient, K; near T_c, $\Delta C/\gamma T_c = 2 \pm 0.5$ for κ-(BEDT-TTF)$_2$CuN(CN)$_2$Br ($T_c \approx 13$ K) but, decreases to 1.6 ±0.2 (closer to the BCS value of 1.46) for (BEDT-TTF)$_2$I$_3$ (T_c=3.4 K);[8] both C_p and K are known accurately for $YBa_2Cu_3O_{7-\delta}$: $\Delta C(T_c)/\gamma T_c \geq 4$ and, $\Delta K_{e,max}(T<T_c)/K_e \approx 3$ to 4;[7a,b] the sharp decrease in τ_1 below T_c (Figure 1b) suggests that α also goes through a maximum below T_c. The competition between AF and superconductivity in the organic metals is similar to that found in superconducting oxides,[6a,b] the exchange fields near 150 K, J_{AF}=130 mT > $J_{spin\text{-}spin} \approx 15$ mT suggest that at these temperatures superconductivity is not allowed by the presence of AF domains in the single crystal, however when the lifetime τ_{AF} of the latter decreases below 10^{-10}s (indicated by the increase in the AF resonance line widths near 44 K in Figure 1a) superconductivity maybe allowed and appears near 10 K. T* half field ESR absorption is also observed in superconducting cuprates single crystals and ceramics near and below T_c,[2] but D ESR is always absent, suggesting that k_1 in (4) is shorter than 10^{-10}s, i.e., the activation energy ΔU in (5) is lower for the latter. ΔU for polaron tunneling decreases as the bond polarizability increases and this increases with the bond order; in the organic conductor the intermolecular S-S bond order is 10^{-3} and in the cuprate superconductors the O-O bond order in the CuO_2 plane is 10^{-2} between sigma bonded O-O pairs at a distance $\langle r_{o\text{-}o}\rangle \cong 0.27$nm,[9] lowering ΔU and, the respective D lifetimes for cuprates below the values for organic metals. The decrease in the bipolaron binding energy for the organic metal (inset Figure 3) with T suggests that as $T \rightarrow J_{spin\text{-}spin} \approx 20$ mK, the T* gap states must contribute to the transport properties as $\frac{1}{2}\Delta_{S\text{-}D} \rightarrow \frac{1}{2}\Delta_{T^*\text{-}D} \rightarrow J_{spin\text{-}spin}$ and, that these transport properties at high magnetic fields (which destroy superconductivity but, lower T* states) will be activated as has been observed in superconducting cuprates.[10] The weak magnetic fields used in the measurement of τ_1 (156 mT) can not destroy the superconductivity.

CONCLUSIONS

The functional dependence of the D, ESR line shape and width on T identifies at least three temperature regions where different processes lead to the disappearance of D polaron states: at temperatures where AF domains are present, and most probably take part in the dynamic equilibria, the rate processes are activated with $\Delta U \approx 10^2$ K; below 44 K the T* ESR is detected when the lifetime of the AF domains is decreased below the detection limit; the onset of the transition to superconductivity is detected at a much lower temperature, 10 K. The understanding of the processes in the different temperature regions is of some importance for any theory of superconductivity which predicts the formation of a Bose condensate above T_c.[4] A comparison of ESR line widths vs T with the conductivity,[1c] of all the organic conductors will give insight on whether the presence of AF domains limits the lifetime of the D states, causing activated transport with $\Delta U \approx 10^2$ K, whether at temperatures when $\Delta U \rightarrow 0$ the formation of T* states are allowed and whether these lead to the superconducting state.

Downloaded by [Tomsk State University of Control Systems and Radio] at 10:08 18 February 2013

Acknowledgment-This work was carried out at SJSU with support from NSF grants DMR 9307387 and INT 9312176.

REFERENCES

1. (a) J.Vivo' Acrivos, P. Hughes and S.S.P. Parkin, J. Chem. Phys. 86, 1780 (1987); (b) S.S.P.Parkin, E.M. Engler, V.Y. Lee and R. Schumaker, Mol. Liq. Cryst. 119, 375 (1985); (c) S.S.P. Parkin conductivity measurements (unpublished)
2. J. V. Acrivos, C. Lei and C.M. Burch, Superlattices and Microstructures, **18**(1995)
3. A. Abragam and B. Bleaney, "Electron Paramagnetic Resonance of Transition Ions", Clarendon Press, Oxford (1970)
4. (a) H. Frölich,"Polarons and Excitons", C.G. Kuper and G.D. Whitfield ed., Plenum Press, N.Y. 1963, p. 1; (b) D. Pines, *ibid*, p.33
5. A.S. Alexandrov and N.F. Mott, International Journal of Modern Physics, B 8, 2075-2109 (1994)
6. (a) J.V. Acrivos, Lei Chen, P. Metcalf, J.M. Honig, R.S. Liu and K.K. Singh, Phys. Rev. B, 50, 13710 (1994); (b). J.V. Acrivos, Lei Chen, C. Jiang, H. Nguyen, P. Metcalf and J.M. Honig, J. Solid State Chem. 111, 343 (1994); (c) F. G. Adrian and D. O. Cowan, Chem. and Eng. News, 70, 40 (1992) and references therein.
7. (a)D.M. Ginsberg, "Physical Properties of High Temperature Superconductors, I", D.M. Ginsberg, ed., World Scientific, New Jersey (1989), p. 1; (b) J.W. Loram and K.A. Mirza, Physica C, 153-155, 1020 (1988); (c) J.L. Tholence, H. Noel, J.C. Levet, M.Potel and P.Gugeon, Solid State Communications, 65, 1131 (1988)
8. (a) B.Andraka, C.S. Jee, J.S. Kim, G.R. Stewart, K.D. Carlson, H.H. Wang, A.V.S. Crouch, A.M. Kini and J.M. Williams, Solid State Comunications, 79, 57 (1991); (b) J. Wosnita X. Liu, D. Schweitzer and H.J. Keller, Phys. Rev. B, 50, 12747 (1994)
9. (a) J.V. Acrivos and O. Stradella, Int. J. of Quantum Mechanics, 46, 55 (1993); (b) Lei Chen, MS Thesis, SJSU (1988)
10. A.P. Mackenzie, S.R. Julian, G.C. Lonzarich, A. Carrington, S.V. Brown and D.C. Sinclair, Phys. Rev. Lett., 71, 1238 (1993)

Downloaded by [Tomsk State University of Control Systems and Radio] at 10:08 18 February 2013